International Journal of Nanomedicine

Dovepress
open access to scientific and medical research

Open Access Full Text Article

ORIGINAL RESEARCH

Trans-resveratrol-loaded nonionic lamellar liquid-crystalline systems: structural, rheological, mechanical, textural, and bioadhesive characterization and evaluation of in vivo anti-inflammatory activity

This article was published in the following Dove Press journal:
International Journal of Nanomedicine
14 September 2017
Number of times this article has been viewed

Bruno Fonseca-Santos*
Cínthia Yuka Satake*
Giovana Maria Fioramonti Calixto*
Aline Martins dos Santos
Marlus Chorilli

School of Pharmaceutical Sciences, São Paulo State University (UNESP), Araraquara, São Paulo, Brazil

*These authors contributed equally to this work

Abstract: Resveratrol (Res) is a common phytoalexin present in a few edible materials, such as grape skin, peanuts, and red wine. Evidence has shown the beneficial effects of Res on human health, which may be attributed to its anti-inflammatory activity. However, the poor aqueous solubility of Res limits its therapeutic effectiveness. Therefore, the use of nanostructured delivery systems for Res, such as liquid-crystalline systems, could be beneficial. In this study, we aimed to develop, characterize, and determine the in vivo effectiveness of Res-loaded liquid-crystalline systems. Systems containing copaiba balsam oil, polyethylene glycol-40 hydrogenated castor oil, and water were designed. Results of polarized light microscopy, small-angle X-ray scattering, texture-profile analysis, and flow-rheology analysis showed that the Res-loaded liquid-crystalline system had a lamellar structure, textural and mechanical (hardness, compressibility, and adhesiveness) properties, and behaved as a non-Newtonian fluid, showing pseudoplastic behavior upon skin application. Furthermore, all liquid-crystalline systems presented bioadhesive properties that may have assisted in maintaining the anti-inflammatory activity of Res, since the topical application of the Res-loaded lamellar mesophase liquid crystals resulted in edema inhibition in a carrageenan-induced paw-inflammation mouse model. Therefore, Res-loaded lamellar mesophases represent a promising new therapeutic approach for inhibition of skin inflammation.

Keywords: lamellar mesophase, liquid crystals, anti-inflammatory properties, topical delivery

Introduction

Skin diseases affect millions of people every day. Inflammatory conditions are known to be the major cause of skin diseases.[1] Topical drug delivery has many advantages over other conventional routes of drug administration,[2,3] because it can provide a noninvasive alternative to the parenteral route.[4] The large surface area of skin and ease of access allows transdermal absorption of drugs.[5]

Several strategies are available to overcome the skin barrier, including the use of penetration enhancers, electroporation, iontophoresis, and nanocarrier systems.[6–11] In this aspect, liquid crystals have been developed for cutaneous delivery of drugs.[12–19] Liquid crystals are systems that can be formed using lipids and amphiphilic molecules, which spontaneously reorganize into three-dimensional structures, such as emulsions, microemulsions, or liquid-crystalline (LC) mesophases (lamellar, hexagonal, and

Correspondence: Marlus Chorilli
School of Pharmaceutical Sciences, São Paulo State University (UNESP), Rodovia Araraquara-Jaú, km 1, Araraquara, São Paulo, 14800-903, Brazil
Email chorilli@fcfar.unesp.br

submit your manuscript | www.dovepress.com
Dovepress
http://dx.doi.org/10.2147/IJN.S138629

cubic), upon contact with water, and these unique internal structures can be loaded with drugs[20] (Figure 1). The lamellar phase is formed from bilayers separated by layers of surfactants and solvents, which form a one- or two-dimensional network. In the hexagonal phase, aggregates are formed by the arrangement of long cylinders that form two- or three-dimensional structures. Lyotropic cubic phases have more complicated structures consisting of a curved, bicontinuous lipid bilayer that extends in three dimensions to generate two interpenetrating but noncontacting aqueous nanochannels.[20] LC systems (LCSs) have been shown to provide sustained release of drug molecules.[21–25]

Resveratrol (Res; trans-3,4′,5-trihydroxystilbene), a phytoalexin found in grapes, red wine, and fruit, is a potent antioxidant and anti-inflammatory agent.[26–30] However, its poor aqueous solubility limits its therapeutic effectiveness. In addition, oral administration of Res is challenging, owing to its low bioavailability in vivo because of its poor solubility, and thus peak plasma levels decrease rapidly.[31–33] Therefore, topical application of Res may be convenient for cutaneous local delivery. However, limited aqueous solubility decreases its topical therapeutic effectiveness, because it decreases its skin penetration.[34]

The use of nanostructured delivery for Res, such as LCSs, could be advantageous, because these systems can be administered easily. In addition, they possess good textural, sensory, and bioadhesive properties. Moreover, they can solubilize both lipophilic and hydrophilic drugs and increase the skin permeation of the drug.[19,25,35] In this study, we aimed to develop, characterize the physicochemical properties, and evaluate the in vivo effectiveness of Res-loaded lamellar LCSs.

Materials and methods

Chemicals and reagents

Copaiba balsam oil, polyethylene glycol (PEG)-40 hydrogenated castor oil, trans-Res with 99.9% purity, and λ-carrageenan were purchased from Sigma-Aldrich (St Louis, MO, USA), PharmaSpecial, (Itapevi, SP, Brazil), Galena (Portland, OR, USA), and Sigma-Aldrich, respectively. Water was purified and deionized using a Milli-Q system obtained from Merck Millipore (Billerica, MA, USA). All other reagents were commercially available and used without further purification.

Ternary-phase diagram

A ternary-phase diagram was constructed point to point using copaiba oil as the oily phase (O) and hydrogenated castor oil as the surfactant (S), in proportions of each component generating 100% of a total formulation. Mixtures of O and S were titrated with deionized water to reach a final amount of 2 g. Then, all vials were heated in a water bath at 45°C with vigorous stirring using a glass rod for 5 minutes. The vials were closed and allowed to stand in the dark for 24 hours at 25°C±0.5°C. Then, they were visually examined, and classified as phase separation (PS), transparent viscous system (TVS), or transparent liquid system (TLS).

Polarized light microscopy

A small amount of the formulations was placed on a glass slide, covered with a coverslip, and examined by polarized light microscopy (PLM) to evaluate the homogeneity of the dispersion and detect the presence of anisotropy. The test was performed at 25°C±0.5°C, and photomicrographs were obtained at magnification of 40×.

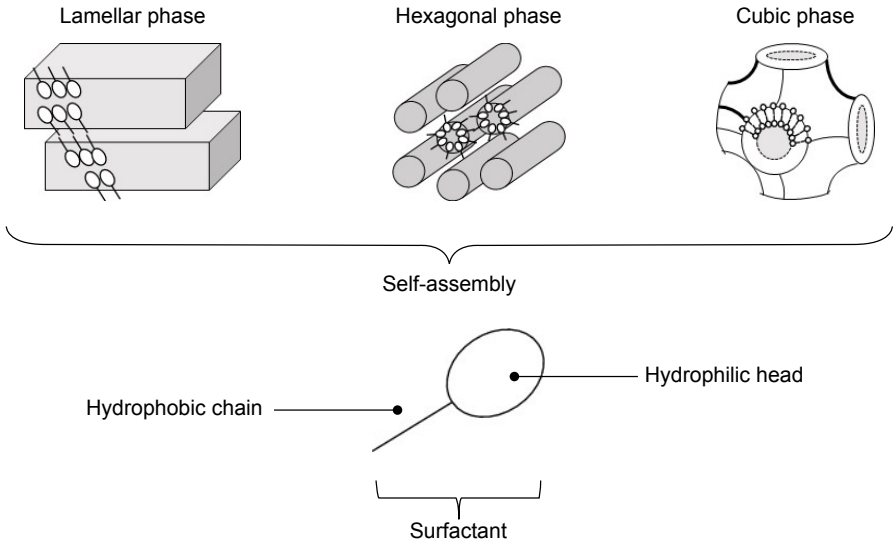

Figure 1 Schematic representation of lamellar, hexagonal, and cubic liquid-crystal mesophases formed by surfactant-molecule self-assembly.

Small-angle X-ray scattering

This test was performed at the National Synchrotron Light Laboratory (LNLS, Campinas, Brazil), using a small-angle X-ray scattering (SAXS)-1 beamline. This beamline was equipped with a monochromator (λ=1.488 Å), Pilatus 300K vertical detector (Dectris, Baden, Switzerland) located 1.5 m from the sample, and a multichannel analyzer to collect SAXS data in a range of q=0.1–5 nm. All measurements were performed at room temperature (20°C–25°C) under the same conditions to calibrate the sample-to-detector distance. Transmission of Kapton tape and mica-sheet corrections was carried out. Parasitic scattering, produced by slits, was subtracted from the total scattering intensity. Analysis time was 30–45 seconds.

Continuous shear (flow) rheology

Flow measurements were carried out using a controlled-stress AR2000 rheometer (TA Instruments, New Castle, DE, USA) with cone–plate geometry (diameter 40 mm, truncation angle 2°, gap, 52 µm) or plate geometry (diameter 40 mm, gap 200 µm) according to the consistency of each formulation. All measurements were carried out in triplicate at 32°C±0.1°C. Samples of the formulations were carefully applied to the lower plate to minimize the shear. Then, they were incubated to equilibrate for 2 minutes prior to analysis. The shear rate ranged from 0 to 100 reciprocal second for the upward curve and from 100–0 reciprocal second for the downward curve for a duration of 120 seconds for each stage, separated by an interval of 10 seconds. Consistency and flow indices were determined from the power law in Equation 1 for quantitative analysis of flow behavior:

$$\tau = k * \gamma^n \quad (1)$$

where τ is the shear stress, γ the shear rate, k the consistency index, and n the flow index.

Texture-profile analysis

Texture-profile analysis (TPA) was carried out to determine the mechanical properties of the formulations, such as hardness, compressibility, adhesion, and cohesion. Samples (50 g) were weighed and placed into 50 mL conical centrifuge tubes (Falcon). Then, they were centrifuged in a Sorvall TC6 centrifuge (Thermo Fisher Scientific, Waltham, MA, USA) at 2,665× g for 4 minutes to ensure uniformity of surface and remove air bubbles. These tubes were then transferred to a thermostatic bath set at 32°C to mimic skin temperature. A TA.XT Plus texture analyzer (Stable Micro Systems, Surrey, UK) was programmed to compress the sample uniaxially at 1 mm/s until a predefined depth (10 mm), and then return to the surface at a speed of 0.5 mm/second. After 5 seconds, a second compression was applied under the same conditions. All samples were analyzed in triplicate.

In vitro evaluation of bioadhesion

Dermatomed pig-ear skin (300 µm) was incubated for approximately 30 minutes in a petri dish containing 0.9% saline solution. The formulations were placed in conical centrifuge tubes, which were maintained in a thermostatic bath at 32°C. Pig-ear skin was fixed with elastic rubber to the cylindrical probe. The cylindrical probe was lowered to allow the skin to be in contact with the sample surface. Contact time was 60 seconds, then the probe was removed. The force required to detach the skin from the sample was determined from the force versus time curve. This experiment was performed in triplicate using texture-analysis equipment.

In vivo evaluation of anti-inflammatory activity

In vivo evaluation was performed in male Swiss mice weighing 25–35 g. The mice were kept in a temperature-controlled environment (22°C) under 12-hour light–dark cycles, and provided with free access to food and water, except during the experiments. The experimental protocol was performed in accordance with the *Guide for the Care and Use of Laboratory Animals*[36] and the ethical principles for animal experimentation established by the Brazilian Committee for Animal Experimentation. This investigation was approved by the animal experimentation ethics committee of the School of Pharmaceutical Sciences, São Paulo State University (protocol CEUA number 71/2015), and complied with international laws.

Mice were subdivided into seven groups (five per group): group I mice were not treated (negative control), group II received topical dexamethasone (positive control), group III received CB-23 formulation without drug, group IV received CB-23R formulation, group V received CB-24 formulation without drug, group VI received CB-24R formulation loaded with Res, and group VII received free Res dissolved in avocado oil.

Paw edema was induced by intraplantar injection of 100 µL of 1% (w:v) λ-carrageenan into the paws of the mice. After 30 minutes, 100 mg of dexamethasone cream or formulation was applied to the paw. After 6 hours, paw diameters were measured using a digital caliper. Data were plotted using GraphPad Prism version 6.0, and one-way

analysis of variance was performed followed by Dunnett's test (α=0.05). Inhibition of edema was calculated:

$$\%\ \text{Inhibition} = \left\{1 - \left[\frac{\text{Test} - \text{Basal}}{\text{Control} - \text{Basal}}\right]\right\} \times 100. \quad (2)$$

Results and discussion

Ternary-phase diagram

Surfactants are amphiphilic molecules that form aggregates in solution. Supramolecular interactions can determine the size and shape of the self-assembled aggregates. Various mesophases, such as micelles, lamellar, bicontinuous, and reverse micelles, can be generated.[37,38] Several studies have shown the ability of amphiphilic molecules, water, and oil to form LC mesophases.[35,39,40]

Figure 2 shows the ternary-phase diagram of water (W), oil (O), and surfactant (S) mixtures. A large region at the upper vertex showed transparent liquid systems (TLSs) with high concentrations of S up to 65%, independent of the O:W ratio. The decrease in the concentration of S, with W and O proportions up to 10 and 70%, respectively, led to the formation of TLSs.

The dilution of the TLS region led to the formation of a viscous system, like a gel, with a proportion of W of 35%–60% and O ratio up to 60%. When S concentration was below 15%, phase separation occurred. Moreover, with the decrease in O and increase in W ratio up to 60%, these regions increased.

Phase behavior showed that we were able to obtain a readily flowing system by combining S, O, and W. In addition, the degree of organization of the system increased when W was added, resulting in a rigid and viscous matrix. This transition could be attributed to the increase in packing and hydration of the hydrophilic heads of S, which reduced the curvature of the interface droplets of the microemulsion.[39] Moreover, the subsequent hydration of S generated a large repulsive force between the head groups, increasing the distances between the lamellar mesophase until a hexagonal mesophase was formed.[41–43]

The different geometries of the amphiphilic molecules and their resultant self-assembled structures that were formed in the presence of a solvent can be understood using the critical packing parameter (CPP) concept.[44] CPP is often defined using Equation 3:

$$\text{CPP} = \frac{v}{a \times l} \quad (3)$$

where v is the volume of the hydrophobic tail, a the polar head-group area, and l the length of the hydrophobic chain of the surfactant.

Hydrocarbon chains tend to associate with each other upon contact with water to minimize their contact with the

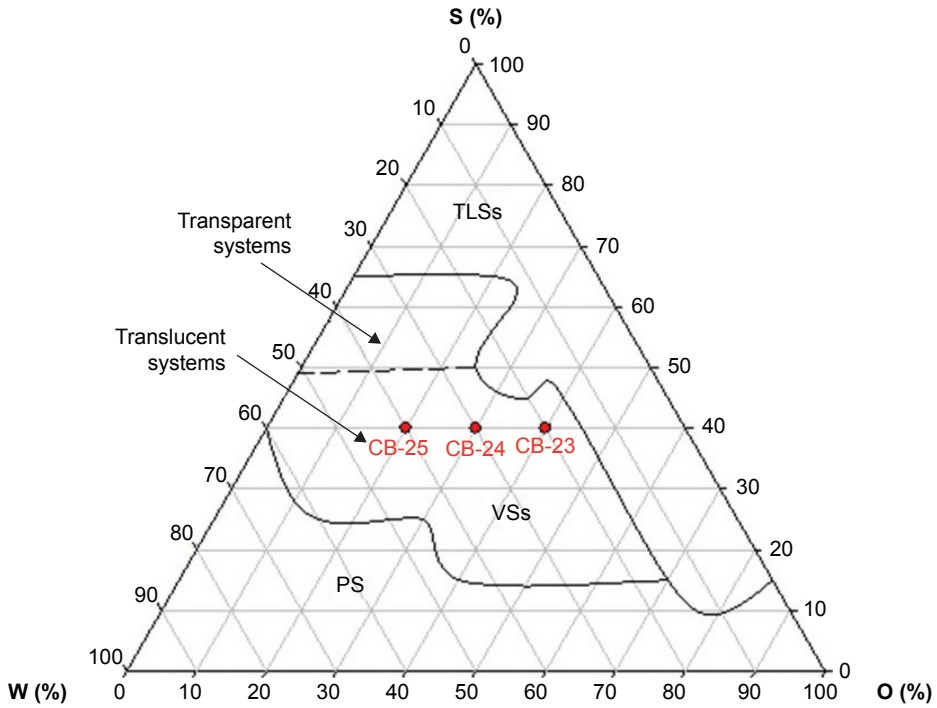

Figure 2 Ternary-phase diagram of copaiba oil as the oily phase (O), hydrogenated castor oil as the surfactant (S), and water (W).
Note: Red points indicate the selected formulations.
Abbreviations: PS, phase separation; VSs, viscous systems; TLSs, transparent liquid systems.

Table 1 Composition of the studied formulations

Formulation	Content (%)		
	Oil phase	Aqueous phase	Surfactant
CB-23	40	20	40
CB-24	30	30	40
CB-25	20	40	40

aqueous phase; therefore, micelles are formed because of both the increased curvature and hydrocarbon chain-packing density.[45] A change in CPP values can roughly predict the order of the surfactant transition associated with the change in the curvature of the water or oil interface.[46] Increasing the number of water molecules increases the CPP value, owing to an increase in the volume of the lipophilic moiety and a reduction in the chain length and head-group area.[47]

Selection of formulations

Transparent or translucent viscous system formations and low-viscosity transparent or translucent system formations were observed over a wide range (Figure 2). These features are important in the design of nanostructured systems for topical application. Certain flow resistance of the formulations is required to facilitate skin-product application. Compositions of the studied formulations are shown in Table 1. Res (0.1%, w:w) was loaded into the oil phase of the formulations. Then, these Res-loaded (CB-23R, CB-24R, and CB-25R) and unloaded (CB-23, CB-24, and CB-25) formulations were characterized by PLM, SAXS, rheological techniques, and bioadhesion studies.

Visual inspection, PLM, and SAXS

Both the translucent visual aspect and viscosity of the formulations were dependent on the water content (Figure 3A). PLM showed that formulations were anisotropic and composed of lamellar LC mesophases, as Malta crosses were observed in all formulations[48] (Figure 3B). Anisotropic materials have optical properties that change with the orientation of the incident light in nonequivalent directions, like the lamellar mesophase. The lamellar phase consists of bilayers that are separated by layers of surfactants and solvents, forming a one- or two-dimensional network.[43] The photomicrographs also showed that the structure of the LC mesophases was not altered by Res loading.

Figure 3C shows the intensity of the scattering patterns and scattering vector modulus (q 1/nm). Curves of SAXS data are shown in Figure 3. Table 2 shows peak position

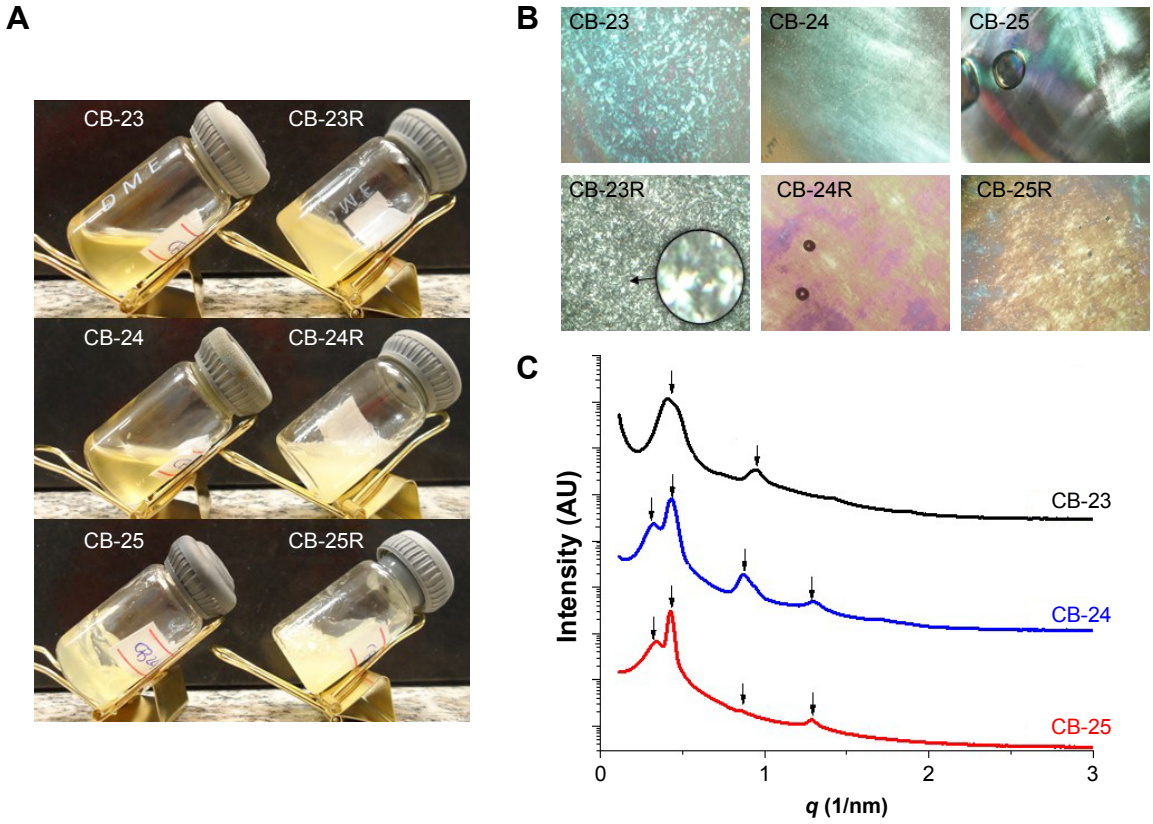

Figure 3 Characterization of the liquid-crystalline dispersions.
Notes: (**A**) Macroscopic appearance, (**B**) photomicrographs obtained by polarized light microscopy (figures were obtained at 40× magnification and the enlarged area at 250× magnification), and (**C**) small-angle X-ray scattering patterns of the samples.

Table 2 Peak positions (*q*) of the SAXS curves, interplanar distances (*d*), and classification of formulations

Formulation	Peak positions *q* (1/nm^{-1})				Peak ratios			*d* (nm)	Mesophase
	q_1	q_2	q_3	q_4	d_2:d_1	d_3:d_2	d_4:d_1		
CB-23	0.47	0.95	–	–	2.0	–	–	14.8	Lamellar
CB-24	0.32	0.42	0.86	1.29	1.31	2.0	4.0	19.6	Lamellar/hexagonal
CB-25	0.32	0.43	0.86	1.29	1.31	2.0	4.0	19.6	Lamellar/hexagonal

Abbreviation: SAXS, small-angle X-ray scattering.

(*q*) values, interplanar distances, and their relationships. For a lamellar LC structure, the relationship between the calculated correlation distances for each Bragg peak follows the ratio 1:2:3.[49–51] Although a peak was found in the SAXS data, no correlation was found with the Bragg distances. We suggest that the formed systems were in transition, suggestive of mixing formation with hexagonal mesophase, for samples CB-24 and CB-25. Similar studies have shown that Res loading into lamellar structures does not affect the structural organization of the mesophase of the system.[51,52] The parameters of the microstructure lattice are represented by the distance between planes (*d*, lamellar structures)[53] and *d*-values were 14–19 nm.

Continuous shear (flow) rheology

Flow data are shown in Figure 4, and mathematical parameters in Table 3. These data showed that all formulations exhibited non-Newtonian flow, because there was no linear relationship between the shear stress and shear rate. Moreover, the flow index showed that all formulations had pseudoplastic flow ($n<1$).[54]

These features are preferable for topical application, because when a force is not applied upon the formulation, ie, when the formulation is kept at rest in the package, it has high viscosity. However, when a force is applied, eg, at the time of application of the formulation on the skin, the formulation viscosity decreases, because the molecules align toward the flow; therefore, the formulation is better spread at the site of action. In addition, after formulation application, ie, when the force application ceases, the formulation has the ability to recover its initial high viscosity, and thus it remains at the site of action for a longer time.[55] As such, the addition of cosurfactants, salts, or other components, such as drugs, may influence the characteristics of LC mesophases, such as viscosity, via interference with the electrostatic interactions or chemical bonds between components of the formulation.[56–58]

It is noteworthy that the incorporation of Res decreased the consistency index (*k*) of all formulations, which demonstrated that this drug affected molecular bonds between formulation components, resulting in a decrease in viscosity. Matos et al[59] reported that emulsions containing Res exhibited viscosities slightly lower than that of the Res-unloaded emulsion. Fujimura et al[52] also observed that Res incorporation decreased the viscosity of an LCS containing silicone glycol copolymer as a surfactant, polyether-functional siloxane as an oily phase, and Carbopol 974P dispersion as an aqueous phase.

Texture-profile analysis

TPA was approved only for the formulations CB-23 and CB-24, because these formulations exhibited mechanical resistance to flow. The CB-25 formulation did not show mechanical resistance to compression; therefore, it was impossible to analyze. TPA results are shown in Table 4.

TPA showed that drug incorporation decreased the mechanical properties of the formulations, including hardness, compressibility, adhesiveness, and cohesiveness. Hardness, compressibility, and adhesiveness showed significant differences ($P<0.05$) between mean values of the different formulations and those of the drug-loaded and unloaded formulations. However, no difference was observed for mean values of cohesiveness ($P>0.05$).

The hardness of materials expresses their resistance to deformation, ie, the maximum force required to cause deformation of a sample.[60] Compressibility is defined as the work required to deform the formulation during the first compression of the probe.[61] The increase in water content and drug loading into the formulation led to the formation of a less packed network, owing to the interpenetration and entanglement into the lamellar mesophase. This phenomenon may have decreased hardness and compressibility values.

Adhesiveness is the work required to overcome the attractive forces between the surface of the sample and the surface of the probe.[61,62] High adhesiveness and cohesiveness of the gel formulations ensure prolonged adhesion of the formulation to the biological surfaces and complete structural recovery following application.[61–63] Certain characteristics are desirable for topical products, including patient acceptability, spreadability, adhesiveness, resistance to rubbing off,

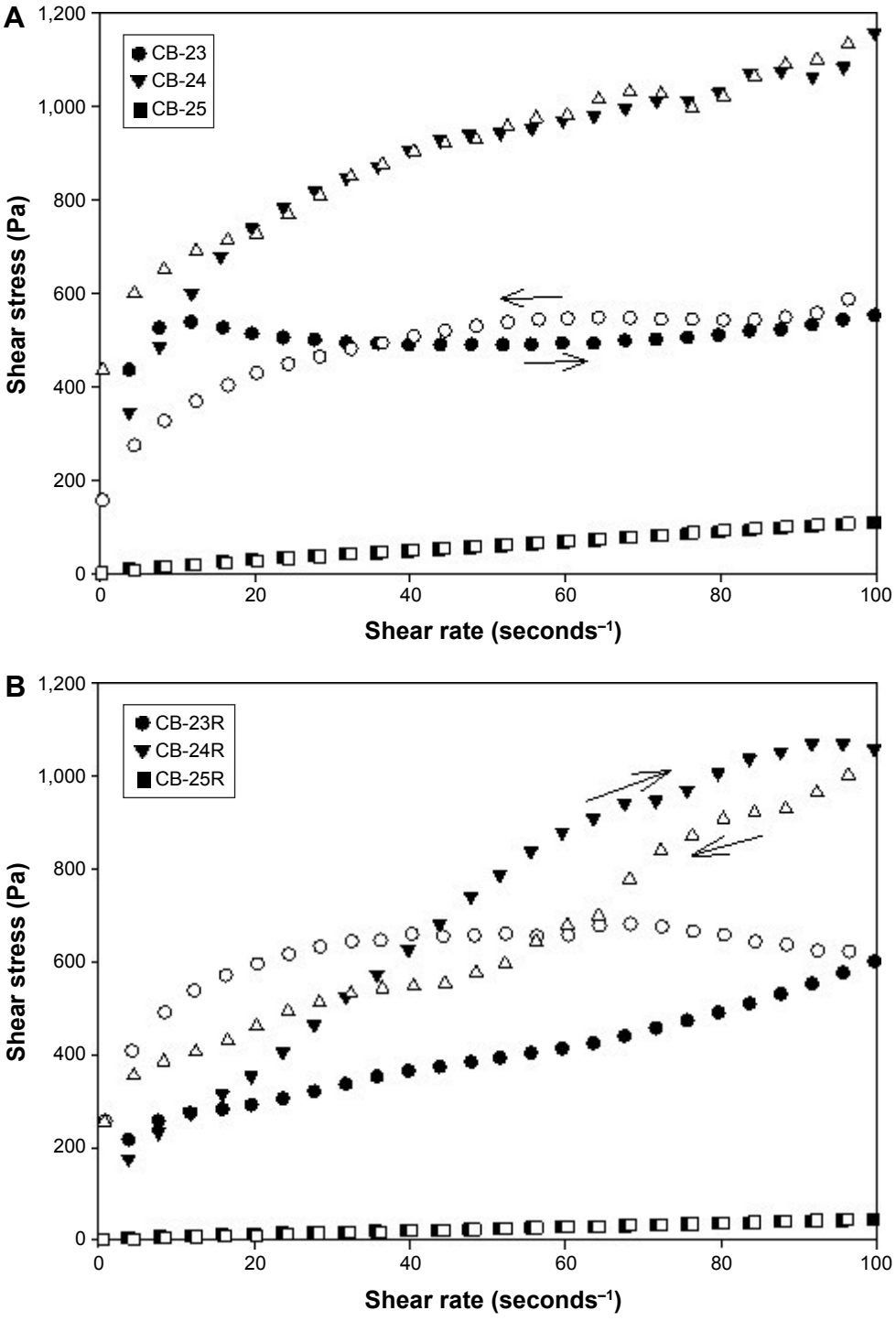

Figure 4 Flow rheograms of unloaded and Res-loaded formulations.
Notes: (**A**) Flow rheograms of unloaded formulations; (**B**) flow rheograms of Res-loaded formulations. The closed symbols represent up curves, and open symbols represent down curves. The standard deviations were omitted for clarity; however, in all cases, coefficients of variation of triplicate analyses were less than 10%. Analysis was carried out at 32°C±0.5°C.
Abbreviation: Res, resveratrol.

capacity to enhance drug release, and (when needed) ability to facilitate drug permeation into the skin.[64–66] Moreover, these mechanical characteristics provide information about the interactions among system components[67] that is important in developing bioadhesive topical formulations.[18]

Bioadhesion studies

Bioadhesive systems are advantageous, because they can prolong the residence time of the drug at the site of application – the skin. This prolonged contact decreases the frequency of application of the product, increases the bioavailability of

Table 3 Flow index (*n*) and consistency index (*k*) of all formulations obtained from the power law (n=3)

Formulations	*n*	*k* (Pa s^n)
CB-23	0.019±0.011	472.270±20.044
CB-23R	0.369±0.026	98.264±10.429
CB-24	0.287±0.012	301.222±15.235
CB-24R	0.645±0.023	58.965±5.685
CB-25	0.826±0.013	2.392±0.136

the drug, and improve the consumer's adherence to product application.[68–70]

Bioadhesive force values are shown in Table 4. Bioadhesive force showed significant differences ($P<0.05$) between mean values of the different formulations and between those of the loaded and unloaded formulations. No difference was observed between CB-25 and CB-25R ($P>0.05$). Drug loading slightly decreased mechanical and bioadhesive properties. As previously reported, addition of water or drug may alter the molecular structure and arrangement of lamellar mesophases.

Polymer dispersions, such as hydrogels, have been studied intensively for skin bioadhesion in topical cutaneous drug delivery,[70–77] and showed good results for bioadhesion.[78–80] The developed LCSs showed similar values, and thus these LCSs are good candidates as topical cutaneous drug-delivery systems, because these amphiphilic systems have shown bioadhesive ability, biocompatibility, and controlled release of drugs.[13,15–19,35,51,52,81–87]

In vivo anti-inflammatory effects

Guest molecules reside in an interconnected network and become part of the nanostructured architecture of the LC matrix.[20,88–90] Biological effects of the nanostructured systems were assessed using biological assays. Res has received considerable attention in several in vitro and in vivo studies, owing to its biological activities, particularly in skin disorders.[29] Furthermore, Res should be delivered to the site of action to attain an ideal response, intensify its therapeutic effects, and reduce its side effects.[30]

The anti-inflammatory effects of the vehicles (CB-23 and CB-24) and loaded formulations (CB-23R and CB-24R) were evaluated in vivo. Figure 5 shows the anti-inflammatory activity of Res incorporated in the lamellar mesophase. The incorporation of Res into LC mesophases affected its intrinsic anti-inflammatory activity, as evidenced by edema inhibition in mouse paws.

The negative control and unloaded formulations showed a statistically significant difference in activity compared to the dexamethasone group ($P<0.01$). No significant difference was observed between free-Res and Res-loaded LCSs ($P>0.05$). The maximal inhibition of inflammation was 63.4%, 27.4%, 42.2%, and 43.1% for dexamethasone, free Res, CB-23R, and CB-24R, respectively. The anti-inflammatory activity of Res-loaded systems was less than that of dexamethasone (0.5%, w:w) as a positive control.

Furthermore, lamellar phases formed by lipids are comparable to the structure of the cell membrane; therefore, they are exploited as model cell membranes.[91] As such, lamellar phases have been used as simple model systems for cell membranes to study the process of membrane fusion.[92,93]

Several assumptions can be made about the mechanism by which the lamellar mesophase affects drug penetration into the skin. First, the structural similarity between this system and skin cells may be responsible for the increase in drug penetration into deep layers of the skin after topical application.[12] Second, the surfactant or oil molecules can diffuse on the skin surface and act as permeation enhancers of Res, because they disrupt the lipid structure of the stratum corneum.[94] This facilitates diffusion across the barrier, which normally limits the penetration of substances. Moreover, this system may increase the solubility of the drug in the skin, which increases the partition coefficient of the drug between the skin and the vehicle.[95,96]

Table 4 Mechanical and bioadhesion properties of the loaded and unloaded formulations (n=3)

Formulation	Mechanical parameters				Bioadhesive force (mN)
	Hardness (mN)	Compressibility (mN/s)	Adhesiveness (mN/s)	Cohesiveness (dimensionless)	
CB-23	599.7±25.0^{a,c}	8,225.0±210.9^{d,f}	6,590.8±284.6^{g,i}	0.817±0.044	94.972±5.646^{j,l,m}
CB-23R	361.3±51.4^{a,c}	4,932.3±75.7^{d,f}	2,234.6±71.3^{g,i}	0.752±0.004	80.565±5.551^{j,l,m}
CB-24	188.3±10.1^{b,c}	2,369.7±227.6^{e,f}	1,627.5±73.9^{h,i}	0.826±0.034	38.648±1.880^{k,l,m}
CB-24R	86.0±1.0^{b,c}	1,366.3±70.8^{d,f}	910.7±3.5^{h,i}	0.737±0.052	20.303±0.319^{k,l,m}
CB-25	*	*	*	*	5.524±0.062^{l}
CB-25R	*	*	*	*	5.021±0.108^{m}

Notes: *It was not possible to collect these data. The same superscript letters indicate statistically significant differences between the means ($P<0.05$).

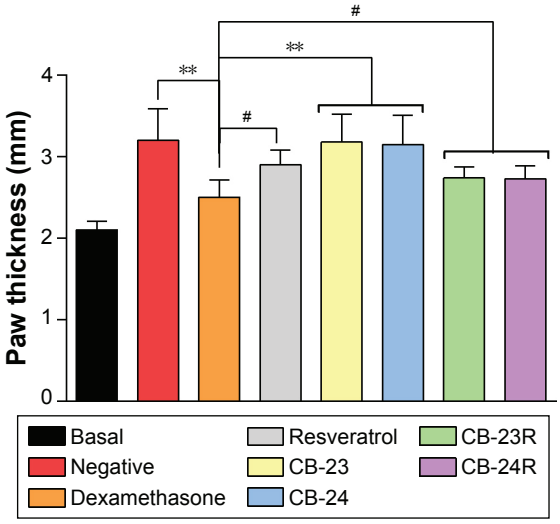

Figure 5 Anti-inflammatory activity of Res-loaded formulations (CB-23R and CB-24R).

Notes: Res-unloaded formulations served as the vehicle, an ointment containing dexamethasone 0.5% (w:w) was used as the positive control, and untreated mice were considered the negative control. Data represent means ± standard deviation of five mice. The statistical significance of the differences in paw thickness between the groups was analyzed using analysis of variance followed by Dunnett's multiple-comparison test. $^{**}P<0.01$; $^{\#}$no significance.

Abbreviation: Res, resveratrol.

Conclusion

It was possible to develop Res-loaded lamellar LCSs containing copaiba balsam oil (20%–40% w:w), PEG-40 hydrogenated castor oil (40% w:w), and purified water (20%–40% w:w). Rheological and TPA data showed that both Res-loaded and unloaded LCSs had proper characteristics for skin administration, such as pseudoplasticity and adhesiveness. Moreover, all LCSs were as bioadhesive as conceptualized bioadhesive formulations, and in particular these LCSs were able to maintain the anti-inflammatory activity of Res. Therefore, it is feasible to conclude that these systems can be used for optimization of drug delivery into the skin for treatment of inflammatory skin diseases.

Acknowledgments

This work was financially supported by the National Council of Technological and Scientific Development (CNPq) in the form of an Initiation Scholarship in Innovation and Technological Development (PIBIT/CNPq) to grantee CYS and regular research grants by the São Paulo Research Foundation (FAPESP) under grant number 14/24180-0. We acknowledge the Brazilian Synchrotron Light Laboratory – LNLS (Campinas, SP, Brazil) staff for the use of their SAXS facilities and Programa de Apoio ao Desenvolvimento Científico (PADC) for their financial support.

Author contributions

All authors contributed toward data analysis, drafting and critically revising the paper, gave final approval of the version to be published, and agree to be accountable for all aspects of the work.

Disclosure

The authors report no conflicts of interest in this work.

References

1. Sigmundsdottir H. Improving topical treatments for skin diseases. *Trends Pharmacol Sci*. 2010;31(6):239–245.
2. Tuan-Mahmood TM, McCrudden MT, Torrisi BM, et al. Microneedles for intradermal and transdermal drug delivery. *Eur J Pharm Sci*. 2013;50(5):623–637.
3. Malik DS, Mital N, Kaur G. Topical drug delivery systems: a patent review. *Expert Opin Ther Pat*. 2016;26(2):213–228.
4. Moore L, Chien YW. Transdermal drug delivery: a review of pharmaceutics, pharmacokinetics, and pharmacodynamics. *Crit Rev Ther Drug Carrier Syst*. 1988;4(4):285–349.
5. Schoellhammer CM, Blankschtein D, Langer R. Skin permeabilization for transdermal drug delivery: recent advances and future prospects. *Expert Opin Drug Deliv*. 2014;11(3):393–407.
6. Hadgraft J. Passive enhancement strategies in topical and transdermal drug delivery. *Int J Pharm*. 1999;184(1):1–6.
7. Prausnitz MR, Langer R. Transdermal drug delivery. *Nat Biotechnol*. 2008;26(11):1261–1268.
8. Hui Z, Yingjie Z, Xiaoye Y, Guangxi Z. Breaking the skin barrier: achievements and future directions. *Curr Pharm Des*. 2015;21(20):2713–2724.
9. dos Santos FK, Oyafuso MH, Kiill CP, Daflon-Gremião MP, Chorilli M. Nanotechnology-based drug delivery systems for treatment of hyperproliferative skin diseases: a review. *Curr Nanosci*. 2013;9(1):159–167.
10. Denet AR, Vanbever R, Préat V. Skin electroporation for transdermal and topical delivery. *Adv Drug Deliv Rev*. 2004;56(5):659–674.
11. Rigon RB, Oyafuso M, Fujimura AT, et al. Nanotechnology-based drug delivery systems for melanoma antitumoral therapy: a review. *Biomed Res Int*. 2015;2015:841817.
12. Estracanholli EA, Praça FS, Cintra AB, Pierre MB, Lara MG. Liquid crystalline systems for transdermal delivery of celecoxib: in vitro drug release and skin permeation studies. *AAPS PharmSciTech*. 2014;15(6):1468–1475.
13. Borgheti-Cardoso LN, Depieri LV, Diniz H, et al. Self-assembling gelling formulation based on a crystalline-phase liquid as a non-viral vector for siRNA delivery. *Eur J Pharm Sci*. 2014;58:72–82.
14. Borgheti-Cardoso LN, Depieri LV, Kooijmans SA, et al. An in situ gelling liquid crystalline system based on monoglycerides and polyethylenimine for local delivery of siRNAs. *Eur J Pharm Sci*. 2015;74:103–117.
15. Borgheti-Cardoso LN, Vicentini FT, Gratieri T, Bentley MV. Liquid crystalline systems containing vitamin E TPGS for the controlled transdermal nicotine delivery. *Braz J Pharm Sci*. 2016;52(1):191–200.
16. Lopes LB, Lopes JLC, Oliveira DCR, et al. Liquid crystalline phases of monoolein and water for topical delivery of cyclosporin A: characterization and study of in vitro and in vivo delivery. *Eur J Pharm Biopharm*. 2006;63(2):146–155.
17. Petrilli R, Eloy JO, Praça FS, et al. Liquid crystalline nanodispersions functionalized with cell-penetrating peptides for topical delivery of short-interfering RNAs: a proposal for silencing a pro-inflammatory cytokine in cutaneous diseases. *J Biomed Nanotechnol*. 2016;12(5):1063–1075.
18. da Silva PB, Calixto GM, Júnior JA, et al. Structural features and the anti-inflammatory effect of green tea extract-loaded liquid crystalline systems intended for skin delivery. *Polymers*. 2017;9(1):30.

19. Fonseca-Santos B, dos Santos AM, Rodero CF, Daflon Gremião MP, Chorilli M. Design, characterization, and biological evaluation of curcumin-loaded surfactant-based systems for topical drug delivery. *Int J Nanomedicine*. 2016;11:4553–4562.
20. Guo C, Wang J, Cao F, Lee RJ, Zhai G. Lyotropic liquid crystal systems in drug delivery. *Drug Discov Today*. 2010;15(23–24): 1032–1040.
21. Drummond CJ, Fong C. Surfactant self-assembly objects as novel drug delivery vehicles. *Curr Opin Colloid Interface Sci*. 1999;4(6):449–456.
22. Shah JC, Sadhale Y, Chilukuri DM. Cubic phase gels as drug delivery systems. *Adv Drug Deliv Rev*. 2001;47(2–3):229–250.
23. Burrows R, Collett JH, Attwood D. The release of drugs from monoglyceride-water liquid crystalline phases. *Int J Pharm*. 1994;111(3): 283–293.
24. Fong WK, Hanley T, Boyd BJ. Stimuli responsive liquid crystals provide 'on-demand' drug delivery in vitro and in vivo. *J Control Release*. 2009;135(3):218–226.
25. de Souza AL, Kiill CP, dos Santos FK, et al. Nanotechnology-based drug delivery systems for dermatomycosis treatment. *Curr Nanosci*. 2012;8(4):512–519.
26. Sengottuvelan M, Deeptha K, Nalini N. Resveratrol ameliorates DNA damage, prooxidant and antioxidant imbalance in 1,2-dimethylhydrazine induced rat colon carcinogenesis. *Chem Biol Interact*. 2009; 181(2):193–201.
27. Karuppagounder V, Arumugam S, Thandavarayan RA, et al. Resveratrol attenuates HMGB1 signaling and inflammation in house dust mite-induced atopic dermatitis in mice. *Int Immunopharmacol*. 2014;23(2): 617–623.
28. Kjær TN, Thorsen K, Jessen N, Stenderup K, Pedersen SB. Resveratrol ameliorates imiquimod-induced psoriasis-like skin inflammation in mice. *PLoS One*. 2015;10(5):e0126599.
29. Pangeni R, Sahni JK, Ali J, Sharma S, Baboota S. Resveratrol: review on therapeutic potential and recent advances in drug delivery. *Expert Opin Drug Deliv*. 2014;11(8):1285–1298.
30. Santos AC, Veiga F, Ribeiro AJ. New delivery systems to improve the bioavailability of resveratrol. *Expert Opin Drug Deliv*. 2011;8(8): 973–990.
31. Cottart CH, Nivet-Antoine V, Laguillier-Morizot C, Beaudeux JL. Resveratrol bioavailability and toxicity in humans. *Mol Nutr Food Res*. 2010;54(1):7–16.
32. Wenzel E, Somoza V. Metabolism and bioavailability of trans-resveratrol. *Mol Nutr Food Res*. 2005;49(5):472–481.
33. Walle T. Bioavailability of resveratrol. *Ann N Y Acad Sci*. 2011;1215(1): 9–15.
34. Yutani R, Morita SY, Teraoka R, Kitagawa S. Distribution of polyphenols and a surfactant component in skin during aerosol OT microemulsion-enhanced intradermal delivery. *Chem Pharm Bull*. 2012;60(8): 989–994.
35. Oyafuso MH, Carvalho FC, Chiavacci LA, Gremião MP, Chorilli M. Design and characterization of silicone and surfactant based systems for topical drug delivery. *J Nanosci Nanotechnol*. 2015;15(1): 817–826.
36. National Research Council. *Guide for the Care and Use of Laboratory Animals*. 8th ed. Washington: National Academies Press; 2010.
37. Tadros T. Liquid crystalline phase. In: *Encyclopedia of Colloid and Interface Science*. Heidelberg: Springer; 2013:682–683.
38. Romsted LS. Introduction to surfactant self-assembly. In: Steed JW, Gale PA, editors. *Supramolecular Chemistry: From Molecules to Nanomaterials*. Hoboken (NJ): Wiley; 2012.
39. Carvalho FC, Campos ML, Peccinini RG, Gremião MP. Nasal administration of liquid crystal precursor mucoadhesive vehicle as an alternative antiretroviral therapy. *Eur J Pharm Biopharm*. 2013;84(1): 219–227.
40. Carvalho FC, Sarmento VH, Chiavacci LA, Barbi MS, Gremião MP. Development and in vitro evaluation of surfactant systems for controlled release of zidovudine. *J Pharm Sci*. 2010;99(5):2367–2374.
41. Mezzenga R. Physics of self-assembly of lyotropic liquid crystals. In: Garti N, Somasundaran P, Mezzenga R, editors. *Self-Assembled Supramolecular Architectures: Lyotropic Liquid Crystals*. Hoboken (NJ): Wiley; 2012:1–20.
42. Chong JY, Mulet X, Boyd BJ, Drummond CJ. Steric stabilizers for cubic phase lyotropic liquid crystal nanodispersions (cubosomes). In: Iglič A, Kulkarni CV, Rappolt M, editors. *Advances in Planar Lipid Bilayers and Liposomes*. Vol 21. Cambridge (MA): Academic Press; 2015:131–187.
43. Garti N, Libster D, Aserin A. Lipid polymorphism in lyotropic liquid crystals for triggered release of bioactives. *Food Funct*. 2012;3(7): 700–713.
44. Israelachvili JN, Mitchell DJ, Ninham BW. Theory of self-assembly of lipid bilayers and vesicles. *Biochim Biophys Acta*. 1977;470(2): 185–201.
45. Ward MD, Horner MJ. Structure and order in soft matter: symmetry transcending length scale. *CrystEngComm*. 2004;6(67):401–407.
46. Malmsten M. *Surfactants and Polymers in Drug Delivery*. Boca Raton (FL): CRC Press; 2002.
47. Li Q. *Nanoscience with Liquid Crystals: From Self-Organized Nanostructures to Applications*. Heidelberg: Springer; 2014.
48. Hyde ST. Identification of lyotropic liquid crystalline mesophases. In: Holmberg K, editor. *Handbook of Applied Surface and Colloid Chemistry*. Hoboken (NJ): Wiley; 2002:299–332.
49. Raman IA, Suhaimi H, Tiddy GJ. Liquid crystals and microemulsions formed by mixtures of a non-ionic surfactant with palm oil and its derivatives. *Adv Colloid Interface Sci*. 2003;106(1–3):109–127.
50. Holmqvist P, Alexandridis P, Lindman B. Modification of the microstructure in poloxamer block copolymer-water-"oil" systems by varying the "oil" type. *Macromolecules*. 1997;30(22):6788–6797.
51. Chorilli M, Prestes PS, Rigon RB, et al. Structural characterization and in vivo evaluation of retinyl palmitate in non-ionic lamellar liquid crystalline system. *Colloids Surf B Biointerfaces*. 2011;85(2): 182–188.
52. Fujimura AT, Martinez RM, Pinho-Ribeiro FA, et al. Resveratrol-loaded liquid-crystalline system inhibits UVB-induced skin inflammation and oxidative stress in mice. *J Nat Prod*. 2016;79(5):1329–1338.
53. Soni SS, Brotons G, Bellour M, Narayanan T, Gibaud A. Quantitative SAXS analysis of the P123/water/ethanol ternary phase diagram. *J Phys Chem B*. 2006;110(31):15157–15165.
54. Chhabra RP. Non-Newtonian fluids: an introduction. In: Krishnan JM, Deshpande AP, Kumar PB, editors. *Rheology of Complex Fluids*. Heidelberg: Springer; 2010:3–34.
55. Junqueira MV, Borghi-Pangoni FB, Ferreira SB, Rabello BR, Hioka N, Bruschi ML. Functional polymeric systems as delivery vehicles for methylene blue in photodynamic therapy. *Langmuir*. 2016;32(1): 19–27.
56. Nakano M, Teshigawara T, Sugita A, et al. Dispersions of liquid crystalline phases of the monoolein/oleic acid/Pluronic F127 system. *Langmuir*. 2002;18(24):9283–9288.
57. Yaghmur A, de Campo L, Sagalowicz L, Leser ME, Glatter O. Emulsified microemulsions and oil-containing liquid crystalline phases. *Langmuir*. 2005;21(2):569–577.
58. Yaghmur A, Kriechbaum M, Amenitsch H, Steinhart M, Laggner P, Rappolt M. Effects of pressure and temperature on the self-assembled fully hydrated nanostructures of monoolein-oil systems. *Langmuir*. 2010;26(2):1177–1185.
59. Matos M, Gutiérrez G, Iglesias O, Coca J, Pazos C. Enhancing encapsulation efficiency of food-grade double emulsions containing resveratrol or vitamin B_{12} by membrane emulsification. *J Food Eng*. 2015;166: 212–220.
60. Jones DS, Woolfson AD, Brown AF. Textural analysis and flow rheometry of novel, bioadhesive antimicrobial oral gels. *Pharm Res*. 1997; 14(4):450–457.
61. Jones DS, Woolfson AD, Brown AF. Textural, viscoelastic and mucoadhesive properties of pharmaceutical gels composed of cellulose polymers. *Int J Pharm*. 1997;151(2):223–233.

62. Jones DS, Woolfson AD, Brown AF, O'Neill MJ. Mucoadhesive, syringeable drug delivery systems for controlled application of metronidazole to the periodontal pocket: In vitro release kinetics, syringeability, mechanical and mucoadhesive properties. *J Control Release*. 1997;49(1):71–79.
63. Bansal K, Rawat MK, Jain A, Rajput A, Chaturvedi TP, Singh S. Development of satranidazole mucoadhesive gel for the treatment of periodontitis. *AAPS PharmSciTech*. 2009;10(3):716–723.
64. Jones DS, Lawlor MS, Woolfson AD. Examination of the flow rheological and textural properties of polymer gels composed of poly(methylvinylether-co-maleic anhydride) and poly(vinylpyrrolidone): rheological and mathematical interpretation of textural parameters. *J Pharm Sci*. 2002;91(9):2090–2101.
65. Ozcan I, Abacı O, Uztan AH, et al. Enhanced topical delivery of terbinafine hydrochloride with chitosan hydrogels. *AAPS PharmSciTech*. 2009;10(3):1024–1031.
66. Hurler J, Engesland A, Kermany BP, Skalko-Basnet N. Improved texture analysis for hydrogel characterization: gel cohesiveness, adhesiveness, and hardness. *J Applied Polym Sci*. 2012;125(1):180–188.
67. Ferreira SB, Moço TD, Borghi-Pangoni FB, Junqueira MV, Bruschi ML. Rheological, mucoadhesive and textural properties of thermoresponsive polymer blends for biomedical applications. *J Mech Behav Biomed Mater*. 2015;55:164–178.
68. Parente ME, Andrade AO, Ares G, Russo F, Jiménez-Kairuz Á. Bioadhesive hydrogels for cosmetic applications. *Int J Cosmet Sci*. 2015;37(5):511–518.
69. Bonacucina G, Cespi M, Misici-Falzi M, Palmieri GF. Rheological, adhesive and release characterisation of semisolid Carbopol/tetraglycol systems. *Int J Pharm*. 2006;307(2):129–140.
70. Carvalho FC, Calixto G, Hatakeyama IN, Luz GM, Gremião MP, Chorilli M. Rheological, mechanical, and bioadhesive behavior of hydrogels to optimize skin delivery systems. *Drug Dev Ind Pharm*. 2013;39(11):1750–1757.
71. Subheet Kumar J, Richa P. Development, characterization and in vivo localization study of topical 5-fluorouracil gels: a comparative study with conventional formulation. *Curr Drug Deliv*. 2014;11(3):401–414.
72. Khan MA, Pandit J, Sultana Y, et al. Novel Carbopol-based transfersomal gel of 5-fluorouracil for skin cancer treatment: in vitro characterization and in vivo study. *Drug Deliv*. 2015;22(6):795–802.
73. Cho CW, Kim DB, Shin SC. Development of bioadhesive transdermal bupivacaine gels for enhanced local anesthetic action. *Iran J Pharm Res*. 2012;11(2):423–431.
74. Guo R, Du X, Zhang R, Deng L, Dong A, Zhang J. Bioadhesive film formed from a novel organic-inorganic hybrid gel for transdermal drug delivery system. *Eur J Pharm Biopharm*. 2011;79(3):574–583.
75. Peppas NA, Bures P, Leobandung W, Ichikawa H. Hydrogels in pharmaceutical formulations. *Eur J Pharm Biopharm*. 2000;50(1):27–46.
76. An NM, Kim DD, Shin YH, Lee CH. Development of a novel soft hydrogel for the transdermal delivery of testosterone. *Drug Dev Ind Pharm*. 2003;29(1):99–105.
77. Shin SC, Kim HJ, Oh IJ, Cho CW, Yang KH. Development of tretinoin gels for enhanced transdermal delivery. *Eur J Pharm Biopharm*. 2005;60(1):67–71.
78. Carvalho FC, Bruschi ML, Evangelista RC, Gremião MP. Mucoadhesive drug delivery systems. *Braz J Pharm Sci*. 2010;46(1):1–17.
79. Machida Y, Nagai T. Bioadhesive preparations as topical dosage forms. In: *Bioadhesive Drug Delivery Systems*. Boca Raton (FL): CRC Press; 1999:641–658.
80. Horstmann M, Müller W, Asmussen B. Principles of skin adhesion and methods for measuring adhesion of transdermal systems. In: *Bioadhesive Drug Delivery Systems*. Boca Raton (FL): CRC Press; 1999:175–195.
81. de Silva HR. Surfactant-based transdermal system for fluconazole skin delivery. *J Nanomed Nanotechnol*. 2014;5(5):1000231.
82. Oliveira MB, do Prado AH, Bernegossi J, et al. Topical application of retinyl palmitate-loaded nanotechnology-based drug delivery systems for the treatment of skin aging. *Biomed Res Int*. 2014;2014:632570.
83. Cintra G, Pinto L, Calixto G, et al. Bioadhesive surfactant systems for methotrexate skin delivery. *Molecules*. 2016;21(2):E231.
84. Liang X, Chen YL, Jiang XJ, Wang SM, Zhang JW, Gui SY. HII mesophase as a drug delivery system for topical application of methyl salicylate. *Eur J Pharm Sci*. 2017;100:155–162.
85. Carvalho AL, Silva JA, Lira AA, et al. Evaluation of microemulsion and lamellar liquid crystalline systems for transdermal zidovudine delivery. *J Pharm Sci*. 2016;105(7):2188–2193.
86. Kadhum WR, Todo H, Sugibayashi K. Skin permeation: enhancing ability of liquid crystal formulations. In: Dragicevic N, Maibach HI, editors. *Percutaneous Penetration Enhancers: Chemical Methods in Penetration Enhancement – Drug Manipulation, Strategies, and Vehicle Effects*. 2015:243–253.
87. Uchino T, Murata A, Miyazaki Y, Ok T, Kagawa Y. Glyceryl monooleyl ether-based liquid crystalline nanoparticles as a transdermal delivery system of flurbiprofen: characterization and in vitro transport. *Chem Pharm Bull*. 2015;63(5):334–340.
88. Sagalowicz L, Mezzenga R, Leser ME. Investigating reversed liquid crystalline mesophases. *Curr Opin Colloid Interface Sci*. 2006;11(4):224–229.
89. Amar-Yuli I, Libster D, Aserin A, Garti N. Solubilization of food bioactives within lyotropic liquid crystalline mesophases. *Curr Opin Colloid Interface Sci*. 2009;14(1):21–32.
90. Negrini R, Mezzenga R. pH-responsive lyotropic liquid crystals for controlled drug delivery. *Langmuir*. 2011;27(9):5296–5303.
91. Simons K, Vaz WL. Model systems, lipid rafts, and cell membranes. *Annu Rev Biophys Biomol Struct*. 2004;33:269–295.
92. Siegel DP. The modified stalk mechanism of lamellar/inverted phase transitions and its implications for membrane fusion. *Biophys J*. 1999;76(1):291–313.
93. Siegel DP. Inverted micellar intermediates and the transitions between lamellar, cubic, and inverted hexagonal lipid phases – II: implications for membrane-membrane interactions and membrane fusion. *Biophys J*. 1986;49(6):1171–1183.
94. Pham QD, Björklund S, Engblom J, Topgaard D, Sparr E. Chemical penetration enhancers in stratum corneum: relation between molecular effects and barrier function. *J Control Release*. 2016;232:175–187.
95. Barel AO, Paye M, Maibach HI. *Handbook of Cosmetic Science and Technology*. 2nd ed. Boca Raton (FL): CRC Press; 2005.
96. Williams AC, Barry BW. Penetration enhancers. *Adv Drug Deliv Rev*. 2012;64 Suppl:128–137.